Effect of Reynolds Number on Boattail Drag

David E. Reubush*
NASA Langley Research Center, Hampton, Va.

An investigation has been conducted in the Langley pilot transonic cryogenic tunnel to determine the effects of varying Reynolds number on boattail drag at subsonic speeds. Six boattailed cone-cylinder nacelle models were tested with the jet exhaust simulated by a cylindrical sting. Reynolds number was varied from about 2.6×10^6 to 132×10^6, by changing model length and unit Reynolds number. Boattail pressure coefficient distributions show that increasing Reynolds number tends to make the pressure coefficients in the expansion region more negative and the pressure coefficients in the recompression region more positive. These two effects were compensating, and, as a result, there was little or no effect of Reynolds number on the pressure drag of isolated boattails.

Nomenclature

A_m = maximum cross-sectional area of model
A_β = incremental area assigned to boattail static-pressure orifice for drag integration
C_D = drag coefficient
$C_{D,\beta}$ = boattail pressure drag coefficient, $\left(\sum_{i=1}^{30} C_{p,\beta,i} \cdot A_{\beta,i}\right) / qA_m$
$C_{p,\beta}$ = boattail static pressure coefficients
d_m = maximum diameter of model
L = length of model from nose to beginning of boattail (characteristic length)
ℓ = length of boattail
M = Mach number
M_∞ = freestream Mach number
p_t = freestream total pressure
q = freestream dynamic pressure
R = Reynolds number
T_t = freestream total temperature
x = axial distance aft from start of boattail
ϕ = meridian angle about model axis, clockwise positive facing upstream, 0° at top of model

Introduction

THE state-of-the-art methods of predicting aircraft propulsion system installation drag rely heavily on wind-tunnel simulation of the actual conditions. This is because the drag-producing components of the propulsion system usually are installed in areas where the flowfield is extremely complex. The high afterbody slopes and long boundary-layer runs result in large viscous effects on boattail pressure drag. Recent attention has been focused on scaling effects, particularly the Reynolds number effects on boattail pressure drag. Work by NASA[1-5] has identified possible large effects of Reynolds number on installed boattail drag. In this work, flight tests were conducted utilizing an F-106 which had two research nacelles mounted under the wings. The boattails to be tested were mounted on these nacelles, and the F-106 was flown at various altitudes to obtain boattail pressure drag data over a wide range of Reynolds numbers. In addition to the flight tests, two scale models of the F-106 were tested in the wind tunnel in order to have a comparison between the flight-test results and wind-tunnel results. Typical results of boattail drag as a function of Reynolds number from this investigation are shown in the left of Fig. 1. These data bring up two questions immediately. 1) Are these effects of Reynolds number fundamental to isolated boattail flow or are they due to afterbody installation effects? 2) Are there any simple methods available with which to evaluate these effects? The data and these questions accentuate the need for further research in this area.

Until recently, the maximum Reynolds numbers achievable in wind tunnels were considerably lower than those achieved in flight; therefore flight tests were the only means by which data could be obtained over a significant Reynolds number range. However, the Langley Research Center recently has placed in operation the 13.5 in. Pilot Transonic Cryogenic Tunnel.[6-9] This facility has the capability of operating at stagnation pressures from about 1-5 atm over a stagnation temperature range from about −320°F (78°K) to 170°F (350°K). As a result, significant variations in Reynolds number can be obtained over the tunnel's operating Mach number range from about 0.1-1.2. The tunnel's operating Reynolds number envelope for this investigation is shown in the right of Fig. 1; the bars indicate the wind-tunnel/flight-test range of the previous NASA work.

The unique capabilities of the cryogenic tunnel provide a ready means by which a single model can be tested over a significant range of Reynolds numbers. With this capability available, a simple experiment was devised to determine whether the previously observed phenomenon was fundamental to boattail flow. Hopefully, this experiment would provide insight into the flow phenomena involved. The experiment utilized isolated, sting-mounted, cone-cylinder nacelle models with various boattail geometries which were tested in the cryogenic tunnel primarily at the subsonic Mach numbers of 0.6 and 0.9. Reynolds number, based on the distance from the nose to the beginning of the boattail, varied from about 2.5×10^6 to 106×10^6 at $M=0.6$ and varied from about 3.4×10^6 to 132×10^6 at $M=0.9$. Isolated boattails were tested to eliminate all extraneous effects and thereby isolate the pure effect of Reynolds number on boattail drag. Therefore, the purpose of this paper is to describe and discuss the results of the investigation of the effect of Reynolds number on isolated boattail drag.

Experimental Methods

A generalized sketch of the 1-in (2.54-cm)-diam boattailed cone-cylinder nacelle models used in this investigation is shown in Fig. 2. There were a total of six models: four short models of differing boattail geometry with a length of 8 in. (20.32 cm) from the nose to the start of the boattail (characteristic length) and two long models with a length of 16 in. (40.64 cm) from the nose to the start of the boattail. The boattail geometry of the two long models duplicated the boattail geometry of two of the short models. The four boattail

Presented as Paper 75-63 at the AIAA 13th Aerospace Sciences Meeting, Pasadena, Calif., Jan. 20-22, 1975; submitted Jan. 20,1975; revision received Sept. 18, 1975.

Index categories: Aircraft Aerodynamics (including Component Aerodynamics); Aircraft Powerplant Design and Installation; Aircraft Testing (including Component Wind-Tunnel Testing).

*Aerospace Engineer, High-Speed Aerodynamics Division.

geometries were circular arc with a length-to-maximum-diameter ratio (fineness ratio ℓ/d_m) of 0.8, circular arc with a fineness ratio of 1.77, circular arc-conic with a fineness ratio of 0.96, and contoured with a fineness ratio of 0.95. It should be noted that the two circular arc boattails are scale models of two which have been tested in the Langley 16-ft transonic tunnel,[10] and the circular arc-conic and the contoured boattails are isolated scale models of two which have been wind-tunnel tested in the Lewis 8 × 6-ft supersonic wind tunnel and flight tested on the F-106.[1-5] The models were all sting mounted, with the diameter of the sting being equal to the model base diameter. Thus, the sting simulated the geometry of a jet exhaust plume for a nozzle operating at its design point. The two circular arc boattails and the circular arc-conic boattail had sting-to-maximum-diameter ratios of 0.5, whereas the contoured had a sting-to-maximum-diameter ratio of 0.544. The length of the constant-diameter portion of the stings was such that, based on the work of Cahn,[11] there should be no effect of the sting flare on the boattail pressure distributions. Also, the sums of the boattail and sting lengths (before the flare) were constant [6.70 in. (17.02 cm)] such that the noses of all four of the short models were at the same tunnel station, and similarly for the two long models.

The models were constructed of cast aluminum with stainless-steel pressure tubes cast as an integral part of the model. The tubes were placed in the sand mold in the proper position, the aluminum poured, and the model machined to the proper contours. Each of the models was instrumented with 30 pressure orifices in three rows of 10 orifices each. Although it would have been desirable to have all of the orifices in one row, the fact that the models were only 1 in. (2.54 cm) in diameter, combined with the number of orifices, precluded this possibility.

Figure 3 is a photograph of one of the short models mounted in the cryogenic tunnel. The tunnel has an octagonal test section with slots at the corners of the octagon and is essentially a scale model of the Langley 16-ft transonic tunnel test section.[12] The test medium for the cryogenic tunnel is nitrogen.

Boattail pressure coefficient distributions from this investigation (Fig. 4) provide substantiation that there are no undesired effects in using nitrogen at cryogenic temperatures to achieve high Reynolds number data. In Fig. 4, boattail pressure coefficient distributions for the circular arc-conic boattail at a Mach number of 0.6 and a Reynolds number of about 10.5×10^6 are compared. One distribution was obtained at a stagnation temperature of −249°F (117°K) and a stagnation pressure of about 1.2 atm, and the other distribution was obtained at a stagnation temperature of 100°F (311°K) and a stagnation pressure of about 5 atm. These data show that, not only are the boattail pressure coefficient distributions the same, but the boattail pressure drag coefficients are the same.

As mentioned earlier, two of the boattails tested in the cryogenic tunnel are models of two boattails which had been tested previously in the Langley 16-ft transonic tunnel. Figure 5 presents a comparison of the boattail pressure coefficient distributions for the $\ell/d_m = 0.8$ circular arc boattail obtained both in the cryogenic tunnel and in the 16-ft transonic tunnel at a Mach number of 0.6 at about the same Reynolds number.

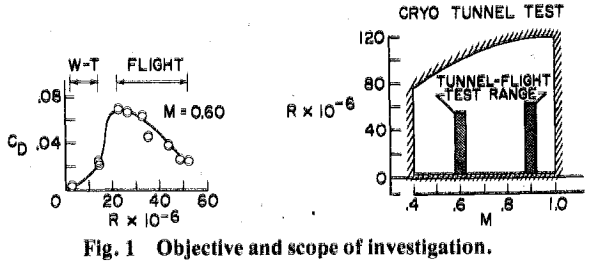

Fig. 1 Objective and scope of investigation.

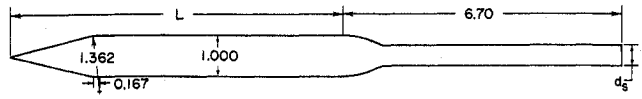

BOATTAIL	L	d_s
CIRCULAR ARC, ℓ/d_m = 0.80	8.00 AND 16.00	0.500
CIRCULAR ARC, ℓ/d_m = 1.77	8.00	.500
CIRCULAR ARC–CONIC	8.00 AND 16.00	.500
CONTOURED	8.00	.544

Fig. 2 Sketch of cone-cylinder nacelle models (all dimensions in inches).

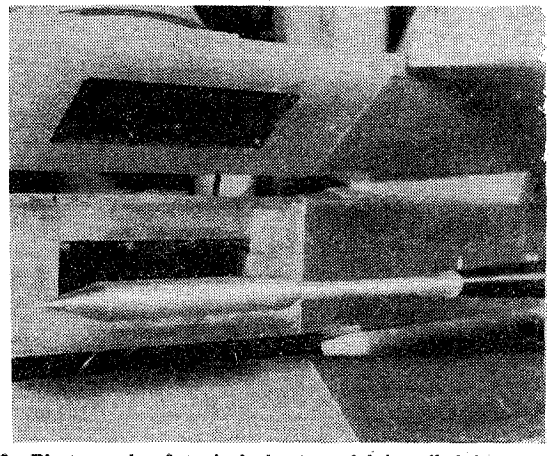

Fig. 3 Photograph of typical short model installed in cryogenic tunnel.

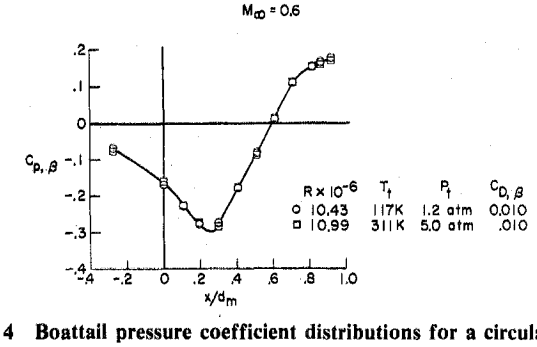

Fig. 4 Boattail pressure coefficient distributions for a circular arc-conic boattail at the same Reynolds number for cryogenic and ambient conditions.

The 16-ft tunnel model was 6 in. (15.24 cm) in diameter and had a tunnel blockage of about 0.1%, whereas the cryogenic tunnel model had a diameter of 1 in. (2.54 cm) and a tunnel blockage of about 0.5%. Within the data scatter, the boattail pressure coefficient distributions are the same in both tunnels, and the integrated boattail pressure drag coefficients agree quite well. This comparison lends a high degree of confidence to the results to be presented.

Results

Experimental Effects of Reynolds Number

Boattail pressure coefficient distributions for the $\ell/d_m = 0.8$ circular arc boattail [8-in. (20.32-cm) model] obtained at four Reynolds numbers from about 7×10^6 to 43×10^6 at a Mach number of 0.6 are shown in Fig. 6. On the cylindrical portion of the model just upstream of the beginning of the boattail, the pressure coefficients at all four Reynolds numbers agree. However, as the flow expands around the shoulder of the boattail, the pressure coefficients at the different Reynolds numbers begin to spread apart such that the higher the Reynolds number, the more negative the pressure coefficients in this expansion region. As the flow begins to recompress over the aft portion of the boattail, the trend is reversed,

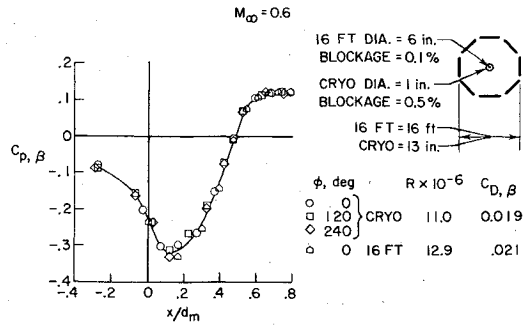

Fig. 5 Comparison of boattail pressure coefficient distributions for a circular arc boattail, $\ell/d_m = 0.8$, obtained in cryogenic tunnel and in 16-ft transonic tunnel.

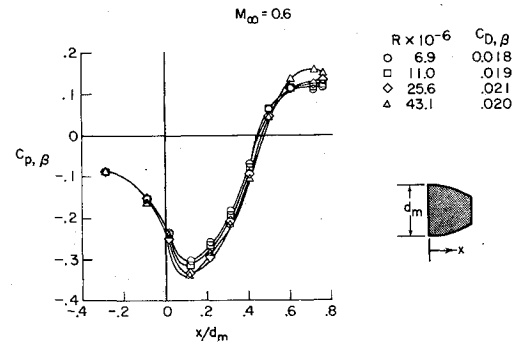

Fig. 6 Boattail pressure coefficient distributions at several Reynolds numbers for a circular arc boattail, $\ell/d_m = 0.8$.

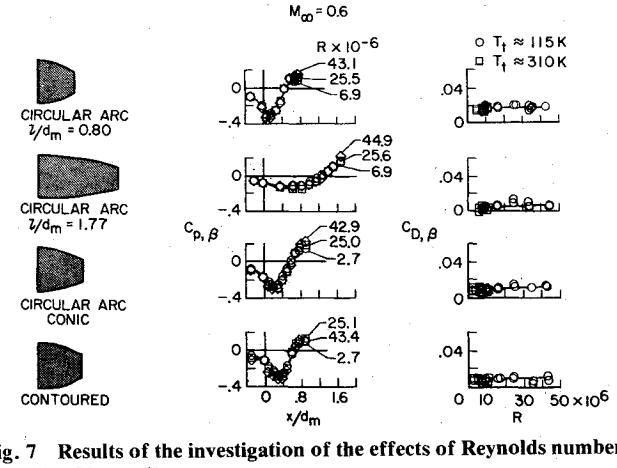

Fig. 7 Results of the investigation of the effects of Reynolds number on isolated boattails.

that is, the higher the Reynolds number, the more positive the pressure coefficients. These two effects are compensating, and, as a result, the integrated boattail pressure drag coefficients are about the same for all four Reynolds numbers.

The result shown in Fig. 6 is typical of that found for all four boattail geometries tested. The pressure coefficient distributions for all four of these boattails show the same trends as previously discussed, (Fig. 7). As Reynolds number is increased, the expansion pressure coefficients become more negative, whereas the recompression pressure coefficients become more positive. As a result, the integrated boattail pressure drag coefficients show no change with Reynolds number. Similar trends in both pressure coefficients and pressure drag coefficients have been reported by Zonars et al.[13]

All data presented in Figs. 6 and 7 were for the short [8-in.(20.32-cm)] models. Similar trends with Reynolds number were observed for the long[16-in. (40.64-cm)] models,

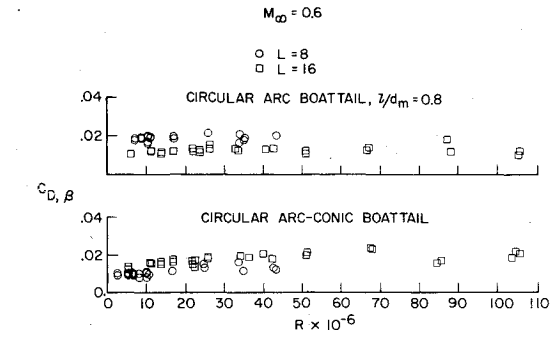

Fig. 8 Boattail pressure drag as a function of Reynolds number for the two boattails tested on both short and long models.

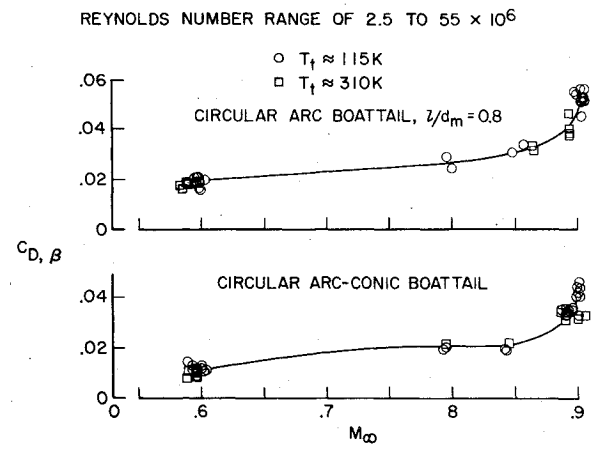

Fig. 9 Effect of Mach number on boattail pressure drag for two boattails (short models) at all Reynolds numbers tested.

both in pressure coefficients and pressure drag coefficients. Boattail pressure drag coefficients as a function of Reynolds number at a Mach number of 0.6 for the two long models, which had the $\ell/d_m = 0.8$ circular arc boattail and the circular arc-conic boattail, are shown in Fig. 8. The boattail drag coefficients for the short models with these boattails are shown for comparison purposes. The slight differences in level between the two models of each boattail are attributed to the fact that the boundary layer at the start of the boattail of each of the long models was, at the same Reynolds number, considerably thicker relative to the model dimensions than that at the beginning of the boattail of the short models.

All data previously presented have been obtained at a Mach number of 0.6, where compressibility effects are relatively small. The effects of Reynolds number on boattail pressure drag also were investigated at $M = 0.9$, where compressibility effects could be large. At this Mach number the boattail pressure coefficients exhibit the same trends as at $M = 0.6$; with increasing Reynolds number the expansion pressure coefficients become more negative and the recompression pressure coefficients become more positive. However, at this Mach number there was a relatively large amount of scatter for some of the boattails when the boattail drag coefficients were plotted as a function of Reynolds number. This scatter can be explained by Fig. 9.

Figure 9 presents the boattail drag coefficients at all Reynolds numbers for the $\ell/d_m = 0.8$ circular arc boattail and the circular arc-conic boattail as a function of Mach number. Both boattails are into the drag rise at a Mach number of 0.9. As a result, a small change in Mach number can have a large effect on the drag coefficient. Since the cryogenic tunnel is a pilot facility, its control systems are relatively unsophisticated, making it difficut to repeat Mach numbers exactly. Therefore, any effect of Reynolds number at this Mach number is obscured by the effect of Mach number. It is

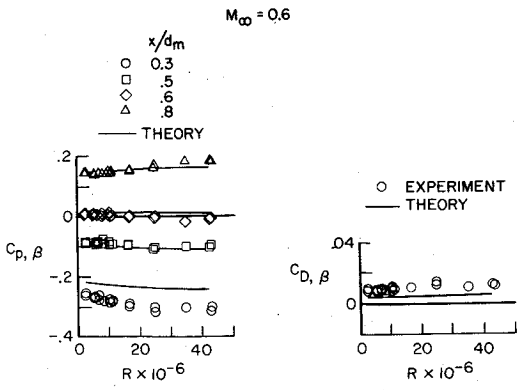

Fig. 10 Comparison of experimentally determined Reynolds number effects with theory.

believed that had Mach number been repeated exactly, the results would be similar to those shown at a Mach number of 0.6, where the drag coefficients for all Reynolds numbers tested were approximately the same.

Comparison with Theory

The trends observed in the behavior of the boattail pressure coefficient distributions and the pressure drag coefficients with Reynolds number are not surprising when compared with the trends predicted by theory. Presented in Fig. 10 are boattail pressure coefficients for the circular arc-conic boattail at various axial stations on the boattail as a function of Reynolds number, with the theoretical predictions shown for comparison. The theory, which is based on the inviscid solution of Hess and Smith[14] with the addition of the boundary-layer displacement thickness from a modified Reshotko-Tucker[15] solution and a separation model based on the work of Presz,[16] predicts both trends: the expansion pressure coefficients becoming more negative and the recompression pressure coefficients becoming more positive with increasing Reynolds number. Also shown in this figure is a comparison of the boattail pressure drag coefficients obtained in the wind tunnel with those predicted by the theory as a function of Reynolds number. Although the value of the drag coefficients predicted by the theory is too low when compared with the experimental results, because the theory underpredicts the peak expansion pressure coefficients on the boattail ($x/d_m = 0.3$), the trend of a slight increase in boattail pressure drag coefficient with increasing Reynolds number is predicted accurately.

Conclusions

The current assessment of the effects of Reynolds number on the pressure distributions and pressure drag of isolated boattails has indicated several significant results. The general effect of increasing Reynolds number tended to make the pressure coefficients more negative in the expansion region and more positive in the recompression region. These two effects were compensating and, as a result, there was little or no effect of Reynolds number on the pressure drag of the isolated boattails. A comparison with theory indicated that these results were caused by the thinning of the boundary layer as Reynolds number increased and the resulting effects of thi the expansion and recompression regions. Therefore, it would seem that based on the results of this investigation, the large effects of Reynolds number observed in the previous NASA work were due to installed nozzle flowfield effects on the boattails and are not fundamental to isolated boattail flow. In order to provide additional information on this phenomenon, work is underway utilizing the pilot cryogenic tunnel to investigate the effects of installed nozzle flowfields on boattail drag over a wide range of Reynolds numbers.

References

[1] Chamberlin, R., "Flight Investigation of 24° Boattail Nozzle Drag at Varying Subsonic Flight Conditions," NASA TM X-2626, 1972.

[2] Chamberlin, R. and Blaha, B. J., "Flight and Wind Tunnel Investigation of the Effects of Reynolds Number on Installed Boattail Drag at Subsonic Speeds, NASA TM X-68162, 1973.

[3] Wilcox, F.A., "Comparison of Ground and Flight Test Results Using a Modified F-106B Aircraft," AIAA Paper 73-1305, Las Vegas, Nev., Nov. 1973.

[4] Chamberlin, R., "Flight Reynolds Number Effects on a Contoured Boattail Nozzle at Subsonic Speeds," NASA TM X-3053, 1974.

[5] Wilcox, F.A., and Chamberlin, R., "Reynolds Number Effects on Boattail Drag of Exhaust Nozzles From Wind Tunnel and Flight Tests," Paper 21, AGARD Conference Preprint 150, 1974.

[6] Goodyer, M.J. and Kilgore, A., "The High Reynolds Number Cryogenic Wind Tunnel," AIAA Paper 72-995, Palo Alto, Calif., Sept. 1972.

[7] Kilgore, R.A., Adcock, J.B., and Ray, E.J., "Flight Simulation Characteristics of the Langley High Reynolds Number Cryogenic Tunnel," *Journal of Aircraft*, Vol. 11, Oct. 1974, pp. 593-600.

[8] Ray, E. J., Kilgore, R. A., Adcock, J. B., and Davenport, E.E., "Test Results From the Langley High Reynolds Number Cryogenic Transonic Tunnel," *Journal of Aircraft*, Vol. 12, June 1975, pp. 539-544.

[9] Polhamus, E.C., Kilgore, R.A., Adcock, J.B., and Ray, E.J., "The Langley Cryogenic High Reynold Number Wind-Tunnel Program," *Astronautics and Aeronautics*, Vol. 12, Oct. 1974, pp. 30-40.

[10] Reubush, D.E., "Experimental Study of the Effectiveness of Cylindrical Plume Simulators for Predicting Jet-On Boattail Drag at Mach Number up to 1.30," NASA TN D-7795, 1974.

[11] Cahn, M.S., "An Experimental Investigation of Sting-Support Effects on Drag and a Comparison With Jet Effects at Transonic Speeds," NACA Rept. 1353, 1958.

[12] Corson, B.W. Jr., Runckel, J.F., and Igoe, W.B., "Calibration of the Langley 16-Foot Transonic Tunnel With Test Section Air Removal," NASA TR R-423, 1974.

[13] Zonars, D., Laughrey, J.A., and Bowers, D.L., "Effects of Varying Reynolds Number and Boundary Layer Displacement Thickness on the External Flow Over Nozzle Boattails," *AGARD Specialists Meeting on Airframe/Propulsion Interference,* Sept. 1974.

[14] Hess, J.L. and Smith, A.M.O., "Calculation of Potential Flow About Arbitrary Bodies," *Progress in Aeronautical Sciences,* edited by D. Kuchemann, Vol. 18, Pergamon Press, London, 1967, pp. 1-138.

[15] "Users Manual for the External Drag and Internal Nozzle Performance Decdeck XI)-Supersonic Flow Analysis (Applicable to Deck VI)," PWA-3465, Suppl. F, Pt. I (Contract No. AF33 (615)-3128), Sept. 1, 1968, Pratt and Whitney Aircraft, East Hartford, Conn.

[16] Presz, W.M., Jr., and Pitkin, E.T., "Flow Separation Over Axisymmetric Afterbody Models," *Journal of Aircraft,* Vol. 11, Nov. 1974, pp. 677-682.